The available heat source influence on the operation of one stage absorption refrigeration systems

Camelia Stanciu, Dorin Stanciu, Michel Feidt, Monica Costea

The available heat source influence on the operation of one stage absorption refrigeration systems.

Camelia STANCIU[1*], Dorin STANCIU[1], Michel FEIDT[2], Monica COSTEA[1]

[1]Department of Engineering Thermodynamics, University Politehnica of Bucharest,
Splaiul Independentei 313, 060042 Bucharest, Romania
[2] L.E.M.T.A., U.R.A. C.N.R.S. 7563, University of Lorraine, Nancy
2, avenue de la Forêt de Haye, B.P.160, 54504 Vandoeuvre Cedex, France
[*](auteur correspondant : Camelia.Stanciu10@yahoo.com)

Résumé – On propose de présenter le fonctionnement d'une installation frigorifique à absorption alimentée par l'énergie thermique fournie par un captateur solaire plan. Le régime de fonctionnement optimum est visé, pour lequel on désire calculer la surface nécessaire du captateur solaire.

Nomenclature

Normal letters

A	area, m^2
E	energy, J
ex	specific exergy, Jkg^{-1}
$\dot{E}x_Q$	heat exergy rate, W
g	gravitational acceleration, ms^{-2}
G	solar radiation density, Wm^{-2}
h	specific enthalpy, Jkg^{-1}
$\dot{m}$	mass flow rate, kg s^{-1}
p	pressure, Pa
$\dot{Q}$	heat flux, W
s	specific entropy, $Jkg^{-1}K^{-1}$
S	entropy, JK^{-1}
$\dot{S}$	entropy rate, WK^{-1}
T	temperature, K
U	overall heat transfer coef., Wm^{-2} K^{-1}
v	specific volume, m^3 kg^{-1}
w	velocity, m s^{-1}
$\dot{W}$	power, W
z	height, m

Greek letters

ξ	ammonia concentration, kg kg^{-1}
τ	time, s

Subscripts

0	restrictive dead state
Ab	absorber / absorbed
C	condenser / solar collector
CV	control volume
f	
gen	generation, creation
i	inlet
L	losses
M	rich solution in ammonia
m	poor solution in ammonia
o	outlet
P	pump
st	storage
T	total
t	tilt
u	useful

1. Introduction

Absorption systems are widely studied, used and many optimization studies are published since they are an eco-friendly alternative to conventional compression chillers. The energy input is no more electrical one, but secondary source (waste) heat is used; solar or geothermal non-conventional sources of energy could be used. On the other hand, absorption units operate with environmental friendly working fluids, so that no contribution to the ozone layer depletion is encountered. The two most used solutions are either bromide lithium – water solution ($LiBr/H_2O$) or the water – ammonia pair (H_2O/NH_3). The first one is the choice for absorption chillers in air conditioning applications due to the high freezing point of the refrigerant (water). The second one is mostly used in refrigerating applications since the refrigerant is ammonia, having a lower vaporization temperature. Such systems could be used for cooling needs and as well for heating ones.

A very useful state of the art on solar absorption refrigeration systems is presented by Kalogirou [1]. Different analysis and numerical simulations have been performed, showing the increase in scientists' interest in this domain. Among them, Ghaddar et al. [2] presented modelling and simulation of a lithium bromide solar absorption system for Beirut. The results showed that a minimum collector area of 23.3 m^2 is required for each ton of refrigeration and an optimum water storage capacity ranges from 1000 to 1500 l so that the studied system operates only on solar energy for 7 h daily.

The present paper presents a comparative thermodynamic analysis of one stage absorption refrigeration systems (ARS), powered by solar energy. The objective of the work is to emphasize the most suitable regime for optimum operation from performances point of view taking into account the solar power collector size (in terms of available heat temperature).

The authors have chosen ammonia-water one stage ARS. Energetic and exergetic analyses are presented and applied for the studied case. Numerical table results and graphical ones are included, putting into evidence the performance improvements from coefficient of performance, exergetic efficiency, entropy generation points of view function on collector size. Sensitivity studies are presented with respect to different decisional parameters. Surprisingly, a high value limit in vapor generator temperature should be imposed for efficient operation. Thus, a constraint arises regarding the solutions for solar power collectors.

2. Research study preparation and purpose

The target of this research is the study of the classical one stage absorption refrigeration system powered by solar energy. By "classical" one means basic configuration for the system to work: absorber, desorber (vapor generator), condenser, evaporator, throttling valves, liquid pump and all necessary connection devices. The studied one stage, single effect, absorption refrigeration system is presented in figure 1. The working fluid in the system is water – ammonia pair (H_2O/NH_3), whose specific properties are determined by the aid of the software Engineering Equation Solver [3].

Thermodynamic modeling is presented, as well as numerical and graphical results regarding its operation in some desired conditions.

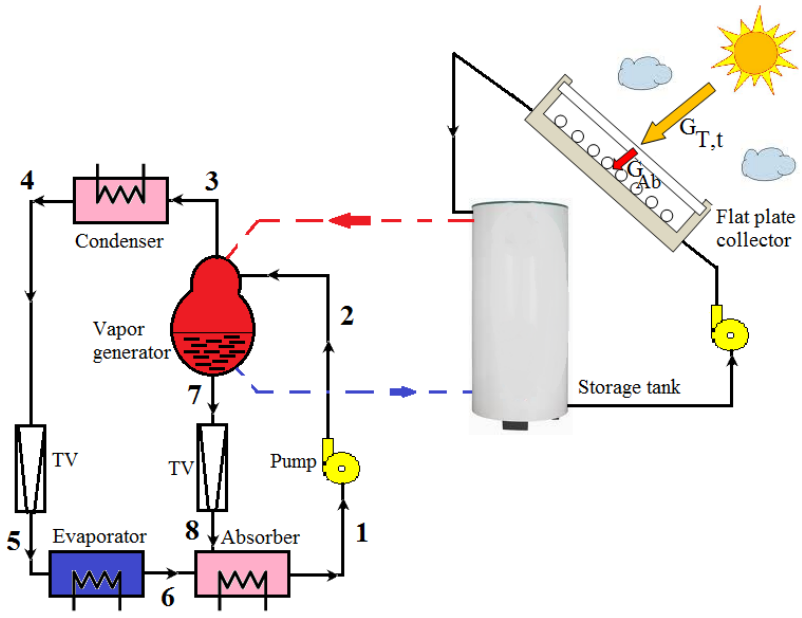

Figure 1 : *Simple effect one stage solar powered absorption refrigeration system*

One may consider the case when both condenser and absorber are cooled by the same water source, so that available cooling water temperature represents a constraint for the condensation and absorber temperatures. More than that, the user needs a certain cooling power and a certain vaporization temperature. Under these operating conditions, one may study the influence of the desorber temperature on the system performances. An optimum value is found, which imposed the solar energy collector size.

Sensitive studies are presented with respect to different decisional parameters, such as: desorber temperature (and thus available heat source) and evaporator temperature for sweeping a large range of utilization cases.

3. Fundamental equations of the mathematical model

The mathematical model consists in applying the First and Second Laws of Thermodynamics for each device of the studied system and all governing equations needed to complete the system of equations in order to solve the problem.

The mathematical expression of the First Law of Thermodynamics for a control volume (CV) is:

$$\frac{dE_{CV}}{d\tau} = \sum_i \left(h + \frac{w^2}{2} + gz \right)_i \dot{m}_i - \sum_o \left(h + \frac{w^2}{2} + gz \right)_o \dot{m}_o + \dot{Q}_{CV} - \dot{W}_{CV} \tag{1}$$

For steady state operation and neglecting the variation of kinetic and potential energies (which is an appropriate assumption for the studied systems), equation (1) becomes:

$$\dot{Q}_{CV} - \dot{W}_{CV} = \sum_o (\dot{m}h)_o - \sum_i (\dot{m}h)_i \tag{2}$$

which is applied to each component of the system.

By applying the Second Law of Thermodynamics to each control volume, one could find the entropy generation in the system:

$$\dot{S}_{gen} = \frac{dS_{CV}}{d\tau} + \sum_o (\dot{m}s)_o - \sum_i (\dot{m}s)_i - \sum_j \left(\frac{\dot{Q}_j}{T_j} \right)_{ext} \tag{3}$$

where $dS_{CV}/d\tau$ is zero for a steady state operation regime; $\dot{Q}_j/T_j$ represents the heat flux $\dot{Q}_j$ exchanged by the system with the surroundings at T_j temperature level.

The exergetic balance equation for a control volume is:

$$\frac{dEx_{CV}}{d\tau} = \sum_j \dot{E}x_{Q_j} - \left(\sum \dot{W} - p_0 \frac{dV}{d\tau} \right) + \sum_i (\dot{m}ex)_i - \sum_o (\dot{m}ex)_o - \sum I \tag{4}$$

which becomes for steady state operation:

$$\sum \dot{I} = \sum_i (\dot{m}ex)_i - \sum_o (\dot{m}ex)_o + \sum_j \dot{E}x_{Q_j} - \sum \dot{W} \tag{5}$$

where the heat exergy rate $\dot{E}x_Q$ is expressed as:

$$\dot{E}x_Q = \dot{Q}\left(1 - T_0 / T_{boundary} \right) \tag{6}$$

In the above equations, the subscript "*0*" denotes the extensive parameters of the system brought in the restrictive dead state. The standard parameters of the environment are: $T_0 = 299.15K$, $p_0 = 1bar$.

Applying all these equations for each component of the system, one may characterize its thermodynamic behavior and forecast a possible improvement of the system operation.

4. Thermodynamic analysis of one stage ARS

Consider the absorption refrigeration system presented in figure 1. The mass flow rate $\dot{m}$ of water-ammonia solution leaves the absorber at concentration ξ (state 1), is pumped to the vapor generator (desorber) (state 2) where a desorption process takes place. The rich ammonia vapors leaving the vapor generator (state 3) are entering the refrigerating part of the system at concentration ξ_M and mass flow rate $\dot{m}_0$, while the remaining poor ammonia solution (state 7) is characterized by a smaller ammonia concentration ξ_m and the remaining mass flow rate $\dot{m} - \dot{m}_0$.

The first step of the thermodynamic modeling is the evaluation of energetic exchanges between the system and surroundings. Thus, equation (3) is applied to each component level, resulting the thermal loads, as presented in table 1 (English sign convention is assumed).

Component	Thermal load	Component	Thermal load
condenser	$\dot{Q}_C = \dot{m}_0(h_4 - h_3)$	*vapor generator*	$\dot{Q}_G = \dot{m}(h_7 - h_2) + \dot{m}_0(h_3 - h_7)$
evaporator	$\dot{Q}_V = \dot{m}_0(h_6 - h_5)$	*absorber*	$\dot{Q}_{Ab} = \dot{m}(h_8 - h_1) + \dot{m}_0(h_6 - h_8)$

Table 1: Thermal loads

At pump level, one may determine the consumed power for pumping the solution in the system; an internal pump efficiency η_P is considered to take into account internal irreversibilities with respect to a reversible adiabatic process:

$$\dot{W}_P = \frac{1}{\eta_P}\dot{m}(p_2 - p_1)v_1 \tag{7}$$

From the mass balance equation in the vapor generator, one may determine the mass flow rate $\dot{m}$ as a function of $\dot{m}_0$ (which is determined from the imposed refrigerating load $\dot{Q}_V$):

$$\xi = \xi_m + \frac{\dot{m}_0}{\dot{m}}(\xi_M - \xi_m) \tag{8}$$

The entropy generation rate in each components of the system is determined by applying equation (3). Results are presented in table 2.

Component	Entropy generation rate	Component	Entropy generation rate
condenser	$\dot{S}_{gen,C} = \dot{m}_0(s_4 - s_3) + \frac{\lvert\dot{Q}_C\rvert}{T_0}$	*absorber*	$\dot{S}_{gen,Ab} = \dot{m}(s_1 - s_8) - \dot{m}_0(s_6 - s_8) + \frac{\lvert\dot{Q}_{Ab}\rvert}{T_{Ab}}$
evaporator	$\dot{S}_{gen,V} = \dot{m}_0(s_6 - s_5) - \frac{\dot{Q}_V}{T_V}$	*vapor generator*	$\dot{S}_{gen,G} = \dot{m}(s_7 - s_2) + \dot{m}_0(s_3 - s_7) - \frac{\dot{Q}_G}{T_G}$
pump	$\dot{S}_{gen,P} = \dot{m}(s_2 - s_1)$	*throttling valves*	$\dot{S}_{gen,TV1} = \dot{m}(s_5 - s_4)$; $\dot{S}_{gen,TV2} = (\dot{m} - \dot{m}_0)(s_8 - s_7)$

Table 2: Entropy generation rates

The overall coefficient of performance and exergetic efficiency, respectively for the studied system are:

$$COP = \frac{\dot{Q}_V}{\dot{Q}_G + \left|\dot{W}_P\right|} \qquad \eta_{Ex} = \frac{\dot{Q}_V\left(\frac{T_0}{T_V} - 1\right)}{\dot{Q}_G\left(1 - \frac{T_0}{T_{Gm}}\right) + \left|\dot{W}_P\right|} \tag{9}$$

It is important to notice that when computing the desorber heat exergy, a mean value for the generator temperature T_{Gm} is used. This mean value is defined as arithmetic mean between temperature values of the states corresponding to the beginning and ending of the evaporating process in the desorber. Significant differences appear when using T_{Gm} instead of $T_{G.}$

Once the system is mathematically modeled, numerical applications could be enabled.

5. Flat plate collector sizing

As the absorption refrigeration cycle is computed, an optimum operation regime is targeted, in terms of minimum entropy generation, respectively maximum exergetic efficiency, as it is presented in Results and discussions section. This regime is obtained by setting the decisional parameters at some specific values. The question now regards the availability of solar radiation density on a flat plate collector (FPC) to ensure the required temperature level inside the vapor generator. The following computational algorithm was used in order to determine this temperature:

- total hourly solar radiation density G_T is computed for a certain location (here Bucharest, at 44.25 North latitude), by summing direct (beam) and diffuse radiation components, as presented in [4][5];

- an optimum tilt angle is computed for the flat plate collector; In June, at Bucharest, this angle was determined to be $\beta = 30°$ (by maximizing the total received radiation density);

- the total solar radiation density on the tilted surface G_{Tl} is than computed, by applying the Liu& Jordan model (isotropic model) [6];

- the absorbed solar radiation by the flat plate collector G_{Ab} is calculated, considering the cover-absorber property in terms of transmittance and absorptance of the FPC, variable with temperature;

- the useful thermal load of the FPC is computed, considering convection and radiation losses through the top of the FPC cover, respectively conduction losses through the FPC insulation [4]; the common value of the overall heat transfer coefficient is $U_L = 5.7W/(m^2K)$ [4] and the mean plate temperature T_{pm} is computed by several iterations:

$$\dot{Q}_u = A_C\left[G_{Ab} - U_L\left(T_{pm} - T_0\right)\right] \tag{12}$$

- than the temperature variation of the fluid inside the FPC (antifreeze solution) is computed, by hourly numerical integration:

$$T_{fo} = T_{fi} + \frac{\dot{Q}_u}{\left(\dot{m}c_p\right)_{FPC}} \tag{12}$$

- a storage tank of 1m^3 water is considered, so the temperature level inside the storage tank T_{st} is computed; convection losses to the exterior are considered too ($(UA)_{st}$=11.1 *W/K*) [4]:

$$\left(\dot{m}c_p\right)_{st}\frac{dT_{st}}{d\tau} = \dot{Q}_u - \dot{Q}_G - (UA)_{st}\left(T_{st} - T_0\right) \tag{12}$$

This temperature level is considered the vapor generator temperature for the ARS.

6. Results and discussions

A numerical simulation is now applied for the above described models for generating results to accomplish the goal of the present paper. A set of numerical input data is considered: the system should accomplish a refrigerating power of 30kW, the ambient temperature is set to 25°C (thus constraining the condensation temperature to 30°C), an internal pump efficiency of 80% is considered. By using EES solver, numerical results are generated. Sensitivity studies are presented in order to make possible an overview on the system operation in a range of possible conditions. Thus, by varying the vapor generator temperature t_G or the vaporization temperature level t_V, one can simulate the system operation in different regimes.

Figure 2a shows the system behavior in terms of *COP* and exergetic efficiency in a range of vapor generator temperature from 80°C to 200°C for a constant vaporization temperature of 0°C. One can notice that a lower limit of t_G is not allowed for system operation since the *COP* drastically decrease; also a higher value deeply decreases the exergetic efficiency. More than that, one can notice that for vapor generator temperatures higher than 120°C, the *COP* variation curve becomes insignificant. Thus, both from energetic (*COP*) and exergetic (η_{Ex}) points of view, a maximum value of t_G should be imposed for good operation. A maximum of η_{Ex} is reached for a value of t_G of about 92°C. The corresponding energetic exchanges (heat fluxes and power) are represented in Figure 2b.

Figure 3a gives an overview on the entropy generation in each component of the system. The highest irreversibilities are generated inside the vapor generator and absorber, as expected. As one can see in figure 3b, the minimum of the total entropy generation $\dot{S}_{gen,tot}$ corresponds to the maximum of the exergetic efficiency, but not necessarily the minimum of each component entropy generation corresponds to the same value. As expected, a lower value for the vaporization temperature is reflected in higher entropy generation. Although, a minimum is reached for each t_V value. This minimum point moves towards higher generator temperatures for lower vaporization temperature values.

In figure 4a one may notice the influence of the available heat source temperature (by means of t_G) for the vapor generator on the exergetic efficiency of the system, with respect to different values set for the vaporization temperature. The first conclusion of these variations is that the maximum value of the exergetic efficiency is reached for lower values of t_V as the generator temperature is increased. At a first glance, one may conclude that for each value of t_V, there is a value of t_G that should be imposed for optimum exergetic efficiency operation. A deeper analysis emphasizes that lowering the t_G value, a better exergetic efficiency is obtained even if it is not an optimum one. For example, when a vaporization temperature t_V =-3°C is required, the maximum exergetic efficiency is reached for a generator temperature t_G =150°C. In fact, a higher value of the exergetic efficiency would be obtained if t_G =100°C, even if this value in not the maximum one for t_G =100°C. So, for a lower temperature in the vapor generator with 33%, one may obtain the same temperature of -3°C in the evaporator with an increase of 29.6% in exergetic efficiency (from 12.5% to 16.2%). This figure gives information about the most suitable generator temperature from exergetic efficiency point of view as a function of the desired vaporization temperature. Let us suppose that for the stated application, the user established the levels of t_V and t_G. Figure 4b gives information on the necessary mass flow rate of solution.

Just as a numerical simulation example, one may consider that the desired operation regime of the ARS is obtained for a generator temperature of 90ºC and a vaporization temperature level of -5 ºC in order to apply the solar calculation model. The working fluid in

the FPC is antifreeze solution having the constant pressure specific heat $c_p = 3900\, J/kgK$; the recommended mass flow rate is $\dot{m} = 0.015kg/s$ for each m^2 of collector area. The collector area A_C is varied for obtaining the minimum necessary value in order to reach 90ºC for the storage tank temperature. By applying the algorithm described in section 5, one obtains the total solar radiation density received by a tilted surface G_{Tt} and absorbed by the FPC (fig 5).

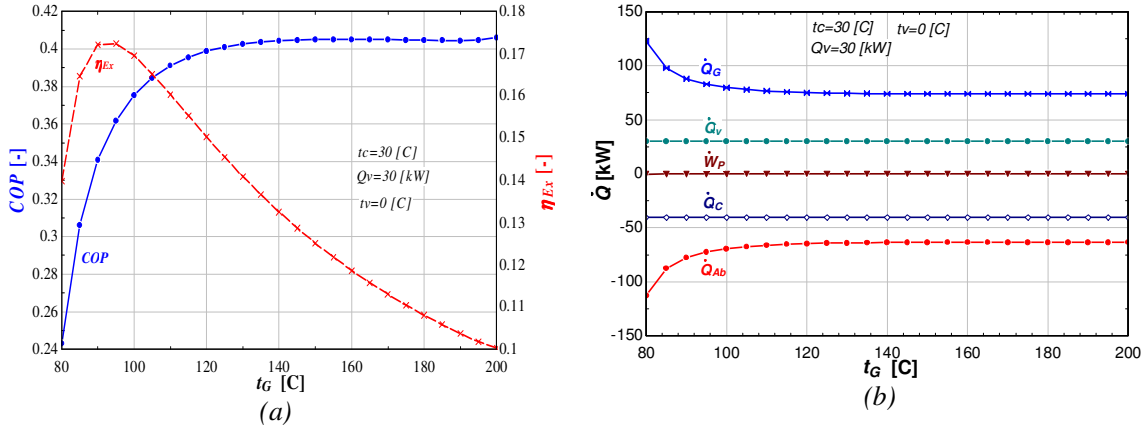

Figure 2 : *COP and exergetic efficiency (a), respectively Energetic exchanges (b) variations with vapor generator temperature t_G for a vaporization temperature level t_V=0 ℃*

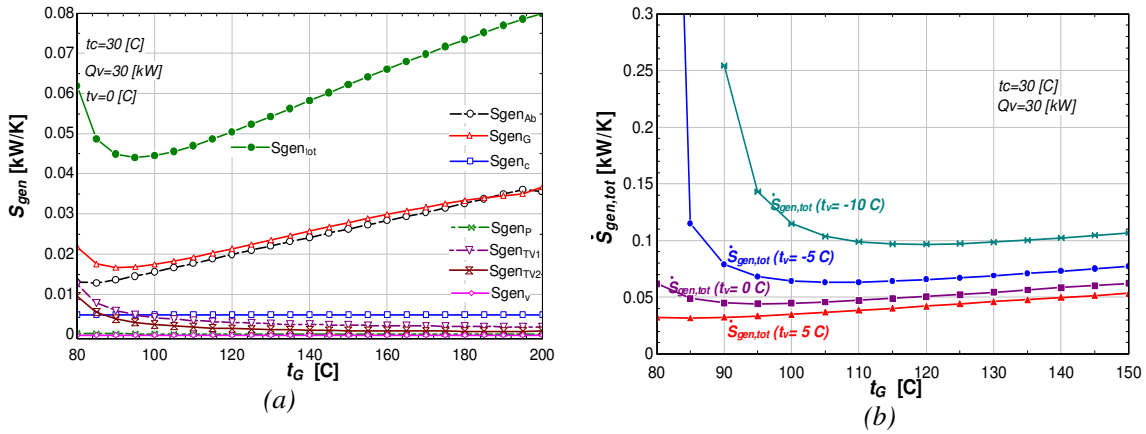

Figure 3 : *Component entropy generation (a) and Total entropy generation (b) variations with vapor generator temperature t_G for a vaporization temperature level t_V=0 ℃ (a) and for different t_V (b)*

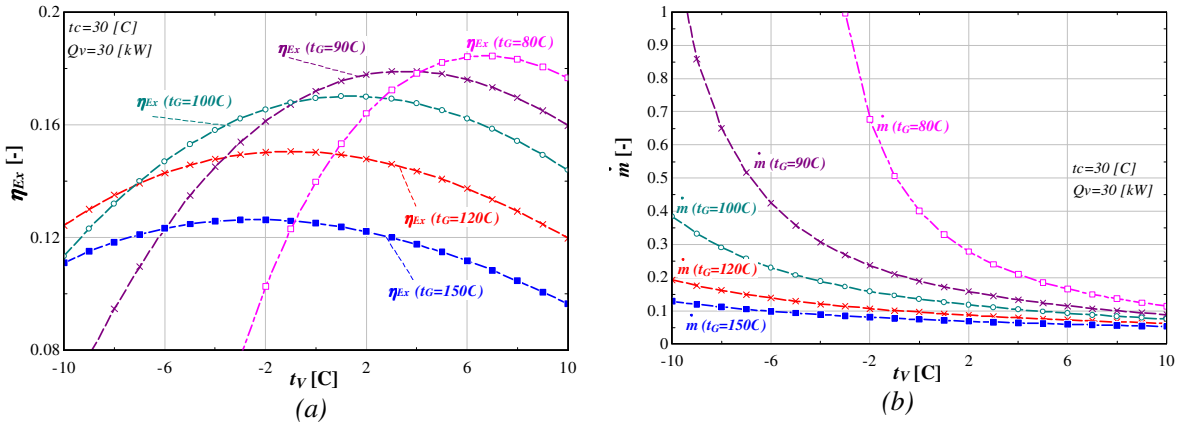

Figure 4: *Exergetic efficiency (a) and Mass flow rate (b) variations with vaporization temperature t_V for different vapor generator temperature levels t_G*

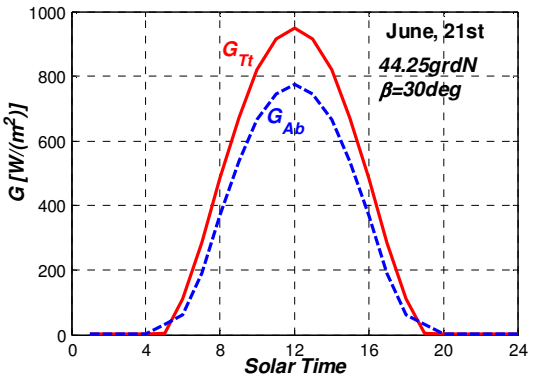

Figure 5: *Total and absorbed solar radiation density*

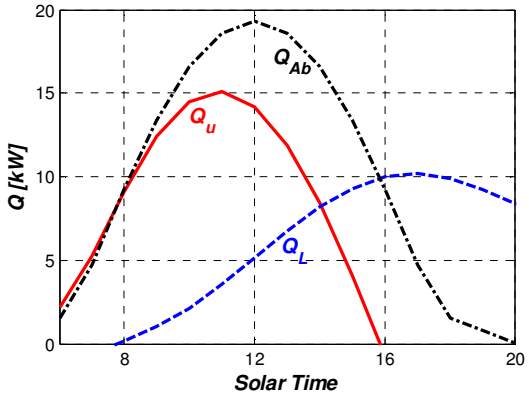

Figure 6: *Absorbed, useful and lost heat fluxes (at flat plate collector level)*

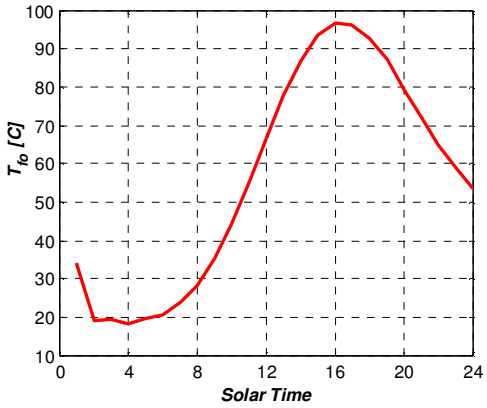

Figure 7: *Fluid temperatures at the inlet and outlet respectively of the FPC and storage tank.*

The associated thermal loads are represented in figure 6. From absorbed solar radiation one computes the absorbed heat flux by the FPC $\dot{Q}_{Ab}$. After several trials, the FPC area A_C was set to 25m^2. The loss heat transfer $\dot{Q}_L$ is represented in figure 6 and the difference is the useful thermal load of the FPC, transferred to the antifreeze solution. The fluid temperature at the outlet of the FPC is represented in figure 7. A maximum value of about 95ºC is reached at noon under the considered conditions. Thus, considering the absorption system operating at 90ºC all day long is not suitable for solar use. According to these results, the ARS operates between 13-20 o'clock and not at optimum parameters and thus a transient model should be further applied (under development).

6. Conclusions

For a given vaporization temperature, there is an optimum generator temperature for which the exergetic efficiency reaches a maximum value. This corresponds to minimum total entropy rate. The same behavior is encountered for an available (constrained) generator temperature, for which there is a certain value of the vaporization temperature that leads to a maximum exergetic efficiency. The paper provides useful nomograms in case of choosing the system parameters in some user-imposed conditions. It is of high interest to know the system behavior under a range of operating regimes, in order to establish an optimum one. The FPC area can be set by applying the above described algorithm.

References

[1] S.A. Kalogirou, Solar thermal collectors and applications, *Progress in Energy and Combustion Science* 30 (2004) 231–295.

[2] NK Ghaddar, M Shihab, F.Bdeir, Modelling and simulation of solar absorption system performance in Beirut, *Renewable Energy*;10(4) (1997) 539–58.

[3] Engineering Equation Solver.

[4] J. Duffie, W. Beckman, Solar engineering of thermal processes, *John Wiley & Sons Inc*, 2006.

[5] D. Stanciu, C. Stanciu, A. Dobrovicescu, A. Gheorghian, Exergy analysis of a solar Stirling engine assembly, *Environmental Engineering and Management J.,* 10(9), 1345-1353 (2011).

[6] B.H. Liu, R.C. Jordan, The interrelationship and characteristic distribution of direct, diffuse and total solar radiation, *Solar Energy,* 4 (3), 1 (1960).